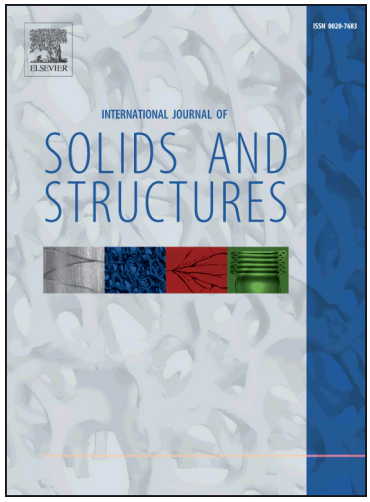

Numerical Simulation of Stress Wave Propagating through Filled Joints by Particle Model

Xiaoling Huang, Shengwen Qi, Ann Williams, Yu Zou, Bowen Zheng

PII: S0020-7683(15)00276-0
DOI: http://dx.doi.org/10.1016/j.ijsolstr.2015.06.012
Reference: SAS 8815

To appear in: *International Journal of Solids and Structures*

Received Date: 11 June 2014
Revised Date: 29 May 2015

Please cite this article as: Huang, X., Qi, S., Williams, A., Zou, Y., Zheng, B., Numerical Simulation of Stress Wave Propagating through Filled Joints by Particle Model, *International Journal of Solids and Structures* (2015), doi: http://dx.doi.org/10.1016/j.ijsolstr.2015.06.012

*Manuscript

Numerical Simulation of Stress Wave Propagating through Filled Joints by Particle Model

Xiaoling Huang[a,b], Shengwen Qi[a]*, Ann Williams[c], Yu Zou[a,b], Bowen Zheng[a,b]

*Corresponding author.

Email address: huangxiaolin@mail.iggcas.ac.cn (Xiaolin Huang), qishengwen@mail.iggcas.ac.cn (Shengwen Qi), ann.williams@beca.com (Ann Williams), zouyu@mail.iggcas.ac.cn (Yu Zou), zhengbowen@mail.iggcas.ac.cn (Bowen Zheng)

a. Key Laboratory of Shale Gas and Geoengineering (KLSGG), Institute of Geology and Geophysics, Chinese Academy of Sciences, Beijing, China, P.O. Box 9825, Chaoyang area, Beijing, 100029, China

b. University of Chinese Academy of Sciences, Beijing, 100049, China

c. Beca Ltd, P O Box 6345, Auckland, New Zealand

ABSTRACT: This paper presents a numerical simulation of stress wave propagation through filled joints using the particle flow code (PFC2D 3.10). A thin layer of granular material without tensile strength is used to model the natural filled joint. The Kelvin viscous-elastic contact model is developed with C++ code and embedded as the dynamic link library in PFC2D 3.10 to simulate the particle deformation behavior of the filled joint. It has been proved that the PFC2D is competent in simulating the stress wave propagating through a filled joint according to the comparison between the forward fitting data and the experiment results. The influence of amplitude and frequency on the transmission coefficient is analyzed, and the results show that the transmission coefficient is amplitude and frequency dependent. Additionally, the effect of the tensile stress wave, loading history and filled thickness on the transmission waves is also evaluated. It has been found that the transmission coefficient decreases with the increase of the filled thickness. The tensile stress wave cannot propagate through the filled joint but can tear apart the filled layer, which weakens the multiple reflections in the filled layer. When the incident wave is composed of multiple pulses, the loading history has an important effect on the transmitted waves. For multiple parallel filled joints, the variation trend of the transmission coefficient versus the dimensionless joint spacing is similar to the analytical result obtained by Zhu et al. (2011) except that the loading mode and amplitudes have an important effect on the magnitude of the transmission coefficient. Finally, the deformation process of the filled layer under different loading modes was examined microscopically.

Keywords: Filled joint; Stress wave; PFC2D; Amplitude- and frequency- dependence; Loading history; Multiple reflections.

1. Introduction

A rock mass generally contains multiple sets of joints which control its mechanical behavior (Goodman, 1976; Sun 1988). The stress wave is often attenuated and slowed when propagating through the joints (King et al., 1986). Predicting the wave attenuation through a jointed rock mass is particularly significant in the safety evaluation of underground geotechnical facilities exposed to seismic and blasting stress waves. To date, most research in this field has been on the seismic response of joints.

Many studies have been conducted on the attenuation of the stress wave propagating through unfilled joints, considering different deformation behaviors, using the displacement discontinuity model (DDM) (Miller,1978; Schoenberg, 1980; Pyrak-Nolte et al., 1990; Zhao and Cai, 2001; Zhao et al., 2006). The DDM assumes that the stress at the front and rear interfaces is continuous but the displacement is not when the stress waves impinge on a joint.

However, the unfilled joint is a special case in nature. Joints are often filled with sand, clay and weathered rock, etc. Theses fillings may be dry, partially saturated or saturated. The fill material may have a thickness of several centimeters, which has a noticeable effect on the mechanical behavior of the rock mass (Barton, 1974; Sinha and Singh, 2000). Therefore, the seismic response of the filled joints should also be studied.

Some experimental studies have been conducted to understand the seismic response of filled joints using the modified Split Hopkinson Pressure Bar (SHPB). Li and Ma (2009) studied the dynamic deformation behavior of filled joints, taking into account different fill thickness and water content. The test results show that under normal dynamic loads, the relationship between the pressure and the closure of the filled joints is nonlinear. Wu et al.,(2012a,b;2013a,b;2014) did

some experimental studies on the dynamic response of joints filled with quartz sands. They found that both displacement and stress are discontinuous when the stress wave impinges on the filled joints. Additionally, the loading rate has an important effect on the seismic response of the filled joint.

Some analytical models were also proposed which assume that the filled joint is an independent element. As can been seen in Fig.1a, the filled joint is often treated as a continuous elastic or viscous-elastic thin layer medium with thickness of L sandwiched between the background rocks (Fehler, 1982; Rokhlin and Wang, 1991; Zhu et al., 2012; Li et al., 2013), which is a direct extension of the layer medium model in seismological theory (Brekhovskikh, 1960; Bedford and Drumheller, 1994). The interfaces in the thin layer medium are often modeled to be welded, which assumes that both the displacement and stress is continuous when the stress wave impinges on the interfaces. For the thin layer medium model, the stress and displacement at the front and rear interface is discontinuous when the stress wave propagates through the filled joint on account of the mass effect of the fill material. Zhu et al. (2011) proposed a displacement and stress discontinuity model (DSDM) to study the seismic response of joints filled with viscous-elastic materials.

Fig.1 (a) the thin layer medium model; (b) schematic view of a natural filled joint

Nevertheless, the thin layer medium model is far from reality when the geological properties of the filled joint are considered. On the one hand, the fill material is often granular, e.g. soil, clay and sand as shown in Fig.1b. Besides the elastic deformation, there is plastic flow in the fill material when loaded. Therefore, the elastic-plastic model is likely to be more suitable to describe the deformation behavior of a filled joint. However, the filled layer usually has no tensile strength.

When tensile stress is applied to the filled joint, the displacement and stress at the front and rear interfaces are discontinuous because of the separation between the background rock and the filled material. Furthermore, the loading/unloading behavior of the filled joint should also be considered. It has been found that the analytical results agree very well with the experimental results only if the loading/unloading effect is considered (Ma et al., 2011; Fan and Wong, 2013).

It is often difficult to establish an analytical model, comprehensively considering all the above aspects. Usually, the numerical simulation is an economical and feasible alternative to study the seismic response of the filled joints. A few numerical simulation studies have been carried out in this field, which mainly address two aspects: the simulation of wave propagation in intact rock and in filled granular materials. In previous studies, particle models based on the discrete element method (DEM) were often applied to simulate wave propagation in the granular medium (Thomas et al., 2009; Zamani and EI Shamy, 2011; Marketos and O'Sullivan, 2013). Particle models were also adopted to simulate the elastic wave propagating through the intact rock (Toomey and Bean, 2000; Resende et al., 2010).

In this paper, numerical simulations are carried out to study the seismic response of filled joints. The particle model is used to model both the hard rock and the filled granular material by making full use of the DEM commercial software of PFC2D 3.10. The Kelvin viscous-elastic contact model is developed with C++ code and embedded as the dynamic link library in PFC2D 3.10 to simulate the particle deformation behavior of the filled joint. Although Zhao et al. (2012) studied the stress wave propagating through the filled joint by the particle manifold method (PMM), it should be noted that the present study differs from that conducted by them. In their study, the filled joint is assumed to be a layer of elastic continuous material which can bear tensile

stress; however in the present study the filled joint is made up of discontinuous granular material that cannot bear tensile stress, and the granular material behaves viscous-elastically when loaded.

2. Verification of PFC2D modeling on wave transmission through a filled joint

To validate the ability of the model to simulate wave transmission through filled joints, the PFC2D results should be first compared with the experimental data.

2.1 Review of previous SHPB tests on wave transmission through a filled joint

Li and Ma (2009) conducted experimental studies on wave propagation through a filled joint by SHPB. The details of the tests are shown in Fig. 2. A filled joint was artificially produced by sandwiching a thin layer of quartz sand between the incident and transmitted granite pressure bars. The input stress wave is excited when a pendulum hammer impinges on the left end of the input bar at a certain velocity. A plastic tube is used to prevent outflow of the sand. Four strain gauges are used to obtain the strain wave signals. The incident and transmitted waves can be extracted after processing the measured wave recordings by the wave separation technique (Li and Ma, 2009; Zhu et al., 2011). Two bars with different lengths of 97 mm and 1005 mm but the same diameter of 50 mm were used as the input and transmitter bars respectively. Both bars have a density of 2,650 kg/m^3 and a P-wave velocity of 4,758 m/s. The quartz sand filling has a density of 1,592.2 kg/m^3. The input and the transmitted waves were recorded at gauges A and A' respectively (see Fig. 2). Thus, the distance between the wave input and receiving points is 965 mm. In this paper, the SHPB test data obtained when the filled joint thickness is 3 mm, the water

content 5% and the swing-angle 40° is selected as the counterpart.

Fig. 2 Details of the Modified SHPB tests conducted by Li and Ma (2009) (a) configuration of the modified SHPB tests; (b) two granite pressure bars and a sand layer sandwiched between the two bars

2.2 Particle model generation and the boundary condition

As mentioned above, the PFC2D was used to carry out the numerical simulation in the present study. For one thing, it has been well proved that the 3D effect can be neglected for the frequency range in the experiment (Li and Ma, 2009). For another thing, the physical experimental setup consisting of two cylindrical rock bars is axisymmetric about the cylindrical central line in the axial direction. Meanwhile, because the filled sand is fine grained and firmly compacted (Li and Ma, 2009), each vertical section through the cylindrical central line should be in analogic conditions. Thus, the setup can be simplified as 2D bar system when modeled by numerical methods. Recently, Li et al. (2014) simulated the real physical SHPB experiment by PFC2D, and the numerical results agree very well with the experimental ones, which proves that the PFC2D can reproduce the real physical SHPB tests. Additionally, it is too heavy to simulate this process with PFC3D due to the limitation of the computing capacity if the setup dimension and particle radius are same as the one in the experiment carried out by Li and Ma (2009) (there will be around 1,767,219 particles for the 3D model), therefore, we adopted PFC2D 3.10 to simulate the seismic response of filled joints at last.

In accordance with the configuration of the modified SHPB tests in Fig.2, a corresponding particle model was established as shown in Fig.3. The procedure employed to generate the particle assembly was adapted from the PFC2D manual (Itasca, 2004). The model has a length of 965mm

and width of 50 mm. In the middle of the model, a layer with thickness of 3 mm is identified as the filled joint with an orange color. The filled layer is composed of 341 particles with radii that vary uniformly between 0.265 and 0.422 mm (average radius is 0.3435 mm). Allowing for the computation capacity of the computer, the disc radii of two bars is taken as a bit larger values that uniformly vary between 0.465 mm and 0.744 mm (average radius is 0.6045 mm). It is reasonable because the grain size of granite is usually greater than 0.5 mm. There are 36,001 particles in all for two bars. Both the rock and the filled layer have the same porosity of 13.7% initially. Four strips of particles are identified with a green color as the four boundaries of the model as shown in Fig.3. The top and bottom boundaries are fixed in the y-direction but free in the x-direction. The incident stress wave is normally applied at the left boundary while the transmitted wave is monitored at the right boundary. When arriving at the left and right truncation boundary, stress waves will reflect back, which makes it difficult to analyze the transmitted waves. Therefore, the viscous non-reflection boundary is used to avoid this kind of interference and ease the extraction of waveforms from the model. In PFC2D, the viscous non-reflection boundary is compiled using the Fish programming language. The basic theory of the viscous non-reflection boundaries is that the boundaries generate a symmetric stress wave to cancel the incoming one when a wave impinges on the boundaries. The symmetric stress wave is related to the average particle velocity $\dot{u}_{ave}$ of the boundary and the P-wave impedance z_p of the medium:

$$\sigma = -z_p \dot{u}_{ave} \tag{1}$$

where, $z_p=\rho V_p$, ρ is the density of the medium and V_p the P-wave velocity.

The static normal stress also needs to be applied to the left and right boundaries. Therefore, the left and right boundaries are actually mixed boundaries in which static and dynamic loadings co-exist

178 with viscous boundaries. The method for implementing mixed boundaries in PFC2D presented by
179 Resende et al. (2010) is adopted in this paper.

180 **Fig. 3 The PFC2D model of the SHPB test**

181 ## *2.3 Forward fitting of the SHPB Test*

182 In PFC2D, particles are assumed to be rigid but can overlap as shown in Fig.4a. The amount
183 of this overlap is dictated by a contact force model. The contact bond and linearly elastic
184 contact-stiff model are employed to model the rock bars. The combination of deformation
185 elements is shown in Fig.4b. In the linearly elastic contact-stiff model, the contact stiffness relates
186 the contact forces and relative displacements in the normal and shear directions. The normal
187 stiffness k_n is a secant stiffness,

188 $$f_n = k_n \cdot u_n \tag{2}$$

189 since it relates the total normal force f_n to the total normal displacement u_n. The shear stiffness k_s
190 is a tangent stiffness,

191 $$\Delta f_s = -k_s \cdot \Delta u_s \tag{3}$$

192 since it relates the increment of shear force to the increment of shear displacement. In the above
193 equations, k_n and k_s denote the normal and shear stiffness, u_n and Δu_s denote the normal
194 displacement and the increment of the shear displacement. Because failure of the rock is not
195 considered in this paper, both normal and shear bond strength are taken as very large values for
196 the discs of the two rock bars.

197 **Fig.4 Schematic of constitutive law of normal and shear contact forces at the interface**
198 **between two discs**

199 It is commonly believed that saturated soil exhibits viscous-elastic deformation behavior

under dynamic loads, and the Kelvin viscous-elastic model (one spring and one dashpot in parallel) is usually adopted to describe this viscous behavior (Verruijt 2009; Das and Ramana 2010). Generally, micro-deformation behavior reflects macro-deformation behavior. Therefore, the disc-disc contact deformation behavior of the filled layer is assumed to satisfy the Kelvin viscous-elastic model. The combination of deformation elements is shown in Fig.4c. The normal component consists of a spring model connected in parallel with a viscous dashpot. The normal force can be expressed as

$$f_n = k_n \cdot u_n + c_n \cdot \dot{u}_n \tag{4}$$

where, c_n denotes the normal viscosity, $\dot{u}_n$ denotes the rate of change of the normal displacement. The combined form of the shear component is the same as the normal one except for the addition of a friction element. When the shear force is less than the friction strength, the increment of the shear force can be expressed as

$$\Delta f_s = -(k_s \cdot \Delta u_s + c_s \cdot \Delta \dot{u}_s)\,. \tag{5}$$

where, c_s denotes the shear viscosity and $\Delta \dot{u}_s$ the rate of change of the shear displacement increment.

When the shear force exceeds the friction strength, the shear force can be expressed as

$$f_s = -f \cdot |f_n| \tag{6}$$

where, f denotes the shear viscosity and friction coefficient.

In PFC2D, a contact model satisfying the above assumptions is not supplied. In accordance with the optional features for writing new contact models (Itasca,2004), we complied a contact constitutive model meeting the assumptions set out above based on a C++ dynamic linked library that is invoked by PFC2D. To verify the reliability of the Kelvin viscous-elastic contact model, a

simple particle model was set up as shown in Fig.5a. The model is made up of two discs with same radius of 0.5m. The bottom one is fixed both in x and y-direction. The top one is fixed only in x-direction. Initially, the two discs are exactly tangent. When the top one is subjected to a constant force f_n, there will be an overlap u_n produced between the two discs as shown in Fig.5a. The analytical expression of u_n can be derived as

$$u_n = \frac{f_n}{k_n}\left(1-\exp\left(-\frac{k_n t}{c_n}\right)\right) \tag{7}$$

where, t denotes time.

Fig.5b shows the comparison between the analytical result and PFC2D result when f_n,= 1.0×10^6 N, k_n=3.0×10^8 N/m and c_n=3.0×10^8 N•s/m. It can be seen that the numerical result is consistent with the analytical one and u_n gradually approaches to $u_0 = f_n / k_n$, which proves that the developed model is reliable.

Fig.5 (a) verified model comprised of two discs; (b) comparison between the analytical result and the PFC2D result.

The synthesized macro-scale material behavior relates to interactions of micro-scale components. However, it is often difficult to choose micro properties so that the behavior of the particle model resembles that of the real material, and the input properties of the microscopic constituents are usually unknown. A feasible method is to select the micro parameters by trial and error until the numerical simulation results match well the experimental data. In order to model the discontinuous granular material, the normal and shear bond strength should be set as 0. Hence, the

particles of the filled layer can produce plastic flow when loaded and remain unrecoverable deformation when unloaded. Moreover, a static normal stress of 2 kPa is applied to the left and right boundaries to make sure that the two bars and filled layer have good contact. Because there is very high inner stress, the filled layer will swell when the bond strength is set as 0. When the static stresses balance, the final porosity of the filled layer is actually 25.04%, not the initial porosity of 13.7%. This is reasonable because the sand fill in the joint has a higher porosity than that of the intact rock. For matching the experimental properties, disc density of the rock and filled layer is taken as 3,070 kg/m^3 and 2,122 kg/m^3 respectively. Thus, the continuum-equivalent density for rock and filled material is 2,650 kg/m^3 and 1,592 kg/m^3, which are the same as the experimental ones.

After lots of trials, the best fit micro-mechanical parameters were selected as shown in Tab. 1. The material properties of the physical experiment and the particle model are compared in Tab.2. Fig. 6 shows the experimental result and the PFC2D result by forward fitting. It can be seen that the PFC2D result agrees approximately with the experimental result. Therefore, the PFC2D is shown to be appropriate for modeling the stress wave transmission through a filled joint. It should be noted that the P-wave velocity of the numerical rock bars is 4,400 m/s which is lower than that of the experimental rock bars. We consider this error range to be generally acceptable.

Table 1 The micro material properties of the particle model

Table 2 Comparison of material properties of the physical experiment and the particle model

Fig. 6 The experimental result and the PFC2D result by forward fitting

3. Parametric studies on stress wave propagating through the filled joint

3.1 Case of one single joint

The transmission coefficient, which is defined as the ratio of the transmitted wave peak value to its incident wave peak value is used to evaluate the wave attenuation. Understanding transmission wave attenuation is important because it can be used to estimate the safety distance when blasting in rock underground. For this reason, this paper focuses on the transmission coefficient. In this section, each parameter will be studied separately while keeping the others constant. Without loss of generality, the sine P-waves are used in the following sections. The configuration of particle models with varied fill thickness is similar to that in Fig.3. All the micro properties and porosity of the particle model are taken as the same as were used in the forward fitting. The same static and viscous boundary conditions are also applied.

Fig. 7 shows the waveforms after half or one cycle of sine waves propagating through a filled joint with a thickness of 3 mm. The incident waves have the same frequency of 5 kHz but varied amplitudes, i.e. 3 m/s in Fig. 7a and 6 m/s in Fig. 7b. It can be found that the transmitted waves only contain the compressive component when one cycle of incident stress waves is applied. This maybe because the filled joint has no tensile strength and cannot bear and pass tensile stress. Hence, there is no tensile component in the transmitted waves. Unlike the case of the unfilled joint which has only one transmitted wave, the whole transmitted wave, in the case of a filled joint, there are several waves arriving at different times. Because the thickness and the initial mass cannot be negligible, multiple reflections occur in the filled thin layer. As a result, there are several waves arriving at different times. When a half cycle of the incident wave is applied, the transmitted wave is composed of more arriving waves than in the case of one cycle. The amplitude of the incident waves also has an important effect on the transmitted waves. An interesting

phenomenon was also identified: that there is effectively only one transmitted wave when one cycle of incident wave has an amplitude of 6 m/s.

Fig. 7 Waveforms after half or one cycle sine stress wave propagating through a filled joint. The amplitudes of the incident waves are (a). 3 m/s and (b).6 m/s.

Fig.8 shows the variation of the transmission coefficient with the amplitudes of the incident wave when the joint thickness is 3 mm and the frequency of the incident wave is 5 kHz. It can be seen that the transmission coefficient depends on the amplitude of the incident wave. When the amplitudes increase, the transmission coefficient becomes large. It changes abruptly when the amplitude is less than 6 m/s. After exceeding that amplitude, it changes gently. Generally, the transmission coefficient of a half cycle of incident wave is larger than that of one cycle. However, the two have essentially the same value when the incident waves have large amplitudes, i.e. 8 m/s.

Fig. 8 Variation of transmission coefficient versus the amplitudes of the incident waves

When underground blasting happens, multiple pulses are produced from the explosion source. The filled joints experience these stress waves in turn. It is therefore important to study the transmission coefficient after multiple pulses propagating through the filled joint. Fig.9 shows the transmitted waveforms from the stress waves consisting of two pulses propagating through a filled joint with a thickness of 3 mm. Each pulse is a half cycle sine wave with the same frequency of 2.5 kHz and amplitude of 2 m/s. Between the two pulses, there are no period in Fig.9a and three cycles of period in Fig.9b. It can be seen that the transmitted waveform in Fig.9a has larger amplitude than that in Fig.9b. Moreover, the period in Fig.9b is so long that the transmitted waveforms arising from the two pulses will not superpose each other. It is commonly believed that the two transmitted waveforms will be the same as in the earlier study based on the thin layer

medium model. However, it is not the case. As shown in Fig.9b, the two transmitted waveforms are obviously different. The above two cases with different periods stand for different loading histories which thus indicates that the loading history has a significant impact on the transmitted waveforms.

Fig. 9 Waveforms after two half cycles of sine pulses with different periods propagating through a filled joint. (a) zero cycles of period; (b) three cycles of period

Fig. 10 shows that the transmission coefficient varies with different periods between two pulses. The thickness of the filled joint is taken as 3 mm. All the pulses have same amplitude of 2 m/s and frequency of 2.5 kHz. It can be found that the transmission coefficient first decreases, then essentially remains invariant with the increment of the period. It suggests that the first and second pulses interact with each other when the period is short. Consequently, the transmission coefficient has large values. Moreover, the shorter the period is, the stronger the interaction is. The value of transmission coefficient increases with decreasing period. However, the interaction of the two pulses becomes unclear when the period is sufficiently long, which makes the transmission coefficient remain invariant.

Fig. 10 Variation of the transmission coefficient with the periods between two pulses

Fig. 11 shows the transmission coefficient of the half cycle of a sine wave propagating through the filled joints with varied thickness. The incident wave has a frequency of 5 kHz and amplitude of 3 m/s and 6 m/s respectively. From Fig.11, it can be seen that the transmission coefficient first decreases abruptly, then gently when the filled thickness gradually increases. When the thickness is very small, i.e. 2 mm, the transmission coefficient approximates 1, which indicates that essentially all the energy can pass through the filled joint.When the filled thickness

331 is less than 4 mm, the amplitudes of the incident waves have little effect on the transmission
332 coefficient. However, the effect of the incident wave amplitudes become clear when the filled
333 thickness exceeds 4 mm.

334 **Fig. 11 Variation of transmission coefficient versus the thickness of the filled joints**

335 Fig.12 shows the transmission coefficient varies with the frequency of the incident waves.
336 The thickness of the filled joint is 3 mm. The incident waves are all half cycle sine waves and
337 have an amplitude of 2 m/s. From Fig.12, it can be seen that the transmission coefficient is
338 frequency dependent. The transmission coefficient decreases sharply when the frequency increases
339 in the range of low values. However, the transmission coefficient varies gradually and finally
340 approximates to 0 when the frequency increases in the range of high values. It indicates that the
341 filled joint can let waves with low frequency pass but stops waves with high frequency.

342 **Fig. 12 Variation of transmission coefficient versus frequency of the incident waves**

343 *3.2 Case of multiple parallel filled joints*

344 As identified in the introduction, a rock mass is usually cut by multiple, sub-parallel planar
345 joints, known as joint sets. Generally a set of joints with nearly identical spacing can be often
346 observed in the field survey (Goodman 1976; Sun 1983). Therefore, it is valuable to study the
347 stress wave propagating through a rock mass with a set of parallel joints. When the stress wave
348 propagates through multiple parallel filled joints, multiple reflections occur between the filled
349 joints, which causes transmission coefficients to vary intricately with the joint spacing (for
350 example Cai and Zhao, 2000; Zhu et al. 2011; Huang et al. 2014). The dimensionless joint spacing,
351 which is defined as the joint spacing divided by the wavelength of the incident wave, has an
352 important influence on the transmission coefficient. Owing to the length limitation of the particle

353 model, only models containing two filled joints are studied. The two filled joints have the same
354 thickness of 3 mm but varied joint spacing between them. The micro-properties and porosity of
355 the particle model are taken as the same as for the forward fitting analysis. The same static and
356 viscous boundary conditions are also applied.

357 Fig.13 shows the variation of transmission coefficient with the dimensionless joint spacing
358 once one or half cycle of incident sine P-waves with the same frequency of 5 kHz and amplitude
359 of 5 m/s propagate through two filled joints. It can be seen that the transmission coefficient first
360 increases slightly with dimensionless joint spacing. After achieving a peak, it decreases instead.
361 Finally, the transmission coefficient is essentially invariant with dimensionless joint spacing. The
362 variation trend described above is similar to the analytical results by Zhu et al. (2011). In their
363 study, the transmission coefficient is approximately the same regardless of whether one cycle or
364 half a cycle of sine wave, when the frequency and amplitude of the incident wave is the same.
365 However, some new phenomena can also be seen in Fig.13. When the dimensionless joint spacing
366 varies in the range of small values, the transmission coefficients in the cases of a half cycle of sine
367 wave and one cycle of sine wave basically have the same magnitudes. After the dimensionless
368 joint spacing reaches the value of 0.1, the transmission coefficient in the case of a half cycle of
369 sine wave is larger than that in the case of one cycle of sine wave. The larger the joint spacing is,
370 the greater their difference is.

371 **Fig.13 Variation of transmission coefficient with dimensionless joint spacing for a half**
372 **and one full cycle of sine P-wave**

373 Fig.14 shows the amplitude effect on the transmission coefficient of half cycle of sine
374 P-waves propagating through two filled joints with different dimensionless joint spacing. The

incident waves have the same frequency of 5 kHz but different amplitude of 3 m/s and 5 m/s. It can be seen that the transmission coefficients under different amplitudes have a similar variation trend with dimensionless joint spacing. The transmission coefficient under large amplitude is larger than that under small amplitude.

Fig.14 Variation of transmission coefficient with dimensionless joint spacing for different amplitudes of transmitted wave

4. Discussion

The thin layer medium models considered in previous studies (Li et al. 2013; Zhu et al. 2012) assume that both the compressive and tensile stress waves can propagate through a filled joint, and moreover, that no plastic deformation occurs in filled joints after bearing the stress wave. In this study, a thin layer of discontinuous granular material was used to model the natural filled joint. In order to better understand the seismic response of filled joints, snapshots at different times in the deformation of the filled joint are shown in Fig.15. The incident waves have the same frequency of 5 kHz and amplitude of 5 m/s but different duration, (i.e. a half cycle for Fig.15a and one cycle for Fig.15b). From Fig.15, it can be observed that the filled layer will be compacted when loaded because plastic flow happens between particles (see Fig.15 at time of 0.21ms). The effective density of the filled material and the stiffness of the filled joints will increase. In the previous study, it was found that the increment of filled density and stiffness can allow more waves to propagate through the filled joint (Zhu et al., 2011). In general, the intensity of the compaction is determined by the amplitude of the incident wave. Therefore, the transmission coefficient is amplitude dependent (see Fig.8).

Fig.15 Snapshots at different times of the deformation of the filled joint (a) a half cycle of

and (b) one cycle of sin P-wave is applied

When the incident wave has duration of one cycle, the contained tensile stress will be applied to the filled layer. Because the filled joint has no tensile strength, the interfaces of the rock bars and the filled layer will be separated gradually, which means they have no interaction (see Fig.15b at time of 0.5ms). As a result, on the one hand, the tensile stress wave is stopped from passing through; on the other hand, the multiple reflections in the filled layer become ambiguous (see Fig.7). The larger the amplitudes of the incident wave are, the more obvious this effect is (see Fig.7b). When the incident wave has only a half cycle duration, there is no tensile stress applied to the filled layer. The interfaces between the rock bars and the filled layer do not separate. Interaction occurs between them. Therefore, the phenomenon of multiple reflections in the case of a half cycle duration is more obvious than that in the case of one cycle duration (see Fig.7).

It can also be found from Fig.15 that the configuration of the filled layer after the stress wave has propagated through (see Fig.15 at time of 0.5ms) is different from the original one (see Fig.15 at time of 0.0 ms). Owing to viscous-elastic plasticity, the deformation of the filled joint depends on the loading history. When subjected to the stress wave, the filled joint responds both by plastic and elastic deformation. Due to the plastic deformation, the seismic properties of the filled joint differ from the initial one. Hence, the transmitted wave produced by the second pulse is different from that produced by the first pulse (shown in Fig. 9b). The phenomena in Fig.10 may be induced by two factors as follows:

The transmitted waves produced by the two pulses superpose each other when the period is short. As the period increases, this superposition gradually fades away. Therefore, the transmission coefficient decreases with the increment of the period. When the period is large

419 enough, the two transmitted waves will not superpose each other at all. Hence, the transmission
420 coefficient remains invariant with the period. Meanwhile, the viscous-elastic deformation of the
421 filled joint cannot recover promptly after reacting to the first pulse because of the effect of the
422 Kelvin viscous-elastic contact model. If the period between two pulses is short, the filled layer still
423 has some unrecovered deformation when the second pulse is arriving. The fill material is still
424 compacted, thus the second pulse can propagate through the filled joint more easily than the first
425 one. In this case, the transmission coefficient has a large value. However, the longer the period is,
426 the more the viscous-elastic deformation can recover. Therefore, the transmission coefficient
427 decreases as the period between pulses increases. When the period is large enough, the elastic
428 deformation can completely recover. At this time, the transmission coefficient is essentially
429 invariant. When one cycle of a stress wave propagates through multiple parallel filled joints,
430 multiple reflections will be weakened because of the effect of the tensile stress wave as mentioned
431 above. Therefore, unlike the previous results, the transmission coefficient in the case of a half
432 cycle of sine wave is larger than that in the case of one cycle of sine wave.
433

434 ## 5. Conclusions

435 Evaluation of attenuation of stress waves propagating through filled joints is of significance
436 in geotechnical engineering applications such as the evaluation of the safety of sub-surface
437 excavations (for example mines or tunnels) exposed to seismic and blasting stress waves. A new
438 Kelvin viscous-elastic contact model has been developed with C++ code in accordance with the
439 optional features of writing new contact models in PFC2D (Itasca, 2004) to model the deformation
440 behavior of fill particles. By making full use of the particle method, a thin layer of

441 viscous-elastic-plastic granular material is used to model the natural filled joint. The filled joint is
442 assumed to have no tensile strength. After a series of numerical simulation studies, some
443 interesting conclusions can be drawn as follows:

444 (1) By comparing the results of the forward fitting and SHPB tests, it is shown that the PFC2D
445 can well simulate a stress wave propagating through a filled joint. Moreover, it is reasonable
446 that the Kelvin viscous-elastic contact model can be used to describe the deformation
447 behavior of the granular fill material.

448 (2) Unlike the case of an open joint, the transmitted wave after propagating through a filled joint
449 consists of more than one wave arriving at different times because of the multiple reflections
450 in the filled layer. The tensile stress wave cannot propagate through the filled joint but can
451 tear apart the filled layer, which weakens the multiple reflections between the background
452 rocks and the filled layer.

453 (3) The transmission coefficient depends on the amplitude of the incident wave. It increases as
454 the amplitude increases. When the amplitude is small, the transmission coefficient of a half
455 cycle of incident wave is larger than that of one cycle. But when the amplitude is sufficiently
456 large, the two have essentially the same values.

457 (4) When the incident wave is composed of multiple pulses, the loading history has a significant
458 effect on the seismic response of the filled joint. Owing to the plastic deformation, the
459 transmitted wave produced by the second pulse is different from that produced by the first one.
460 The transmission coefficient decreases first, then remains invariant as the period between the
461 two pulses increases.

462 (5) The transmission coefficient decreases with the increment of the filled thickness. The filled

joint can let waves with low frequency pass but stop waves with high frequency, which suggests that the transmission coefficient is frequency dependent.

(6) For multiple parallel filled joints, the change law of the transmission coefficient versus dimensionless joint spacing is similar to the analytical result obtained by Zhu et al. (2011) except that the loading mode and amplitudes have an important effect on the magnitude of the transmission coefficient.

6. Acknowledgements

The authors would like to give great thanks to Profs. Li J. C., Ma G.W. and Zhu J. B. for kindly sharing of the experimental data. The authors also would like to acknowledge the anonymous reviewers for their kind suggestions and constructive comments. This research is supported by funds from National Natural Science Foundation of China under Grants Nos. 41322020 and 41172272 and Chinese Academy of Science under Knowledge Innovation Project Grant Nos. KZZD-EW-05-02 and KZCX2-EW-QN108.

References

Barton, N., 1974. A review of the shear strength of filled discontinuities in rock. Norwegian Geotechnical Institute. Publication 105, 1–38.

Bedford, A., Drumheller, D., 1994. Elastic wave propagation. Wiley.

Brekhovskikh, L.M., 1960. Waves in Layered Media. Academic, San Diego.

Cai, J., Zhao, J., 2000. Effects of multiple parallel fractures on apparent attenuation of stress waves in rock masses. Int. J. Rock Mech. Min. Sci. 37, 661-682.

Das, B., Ramana, G., 2010. Principles of soil dynamics. Cengage Learning.

485 Fan, L., Wong, L., 2013. Stress wave transmission across a filled joint with different
486 loading/unloading behavior. Int. J. Rock Mech. Min. Sci. 60, 227-234.
487 Fehler, M., 1982. Interaction of seismic waves with a viscous liquid layer. Bull. Seismol. Soc. Am.
488 72, 55-72.
489 Goodman, R.E., 1976. Methods of geological engineering in discontinuous rocks. West Publishing,
490 St. Paul.
491 Huang, X., Qi, S., Guo, S., Dong, W., 2014. Experimental Study of Ultrasonic Waves Propagating
492 Through a Rock Mass with a Single Joint and Multiple Parallel Joints. Rock. Mech. Rock.
493 Eng. 47, 549-559.
494 Itasca., 2004. PFC2D (Particle Flow Code in 2 Dimensions) Version3.1, Minneapolis.
495 King, M., Myer, L., Rezowalli, J., 1986. Experimental studies of elastic-wave propagation in a
496 columnar-jointed rock mass. Geophys. Prospect. 34, 1185-1199.
497 Li, J., Ma, G., 2009. Experimental study of stress wave propagation across a filled rock joint. Int. J.
498 Rock Mech. Min. Sci.46, 471-478.
499 Li, J.C., Wu, W., Li, H., Zhu, J., Zhao, J., 2013. A thin-layer interface model for wave propagation
500 through filled rock joints. J. Appl. Geophys. 91, 31-38.
501 Li, X., Zou, Y., Zhou, Z., 2014. Numerical simulation of the rock SHPB test with a special shape
502 striker based on the discrete element method. Rock. Mech. Rock. Eng.47, 1693-1709.
503 Ma, G., Li, J., Zhao, J., 2011. Three‐phase medium model for filled rock joint and interaction
504 with stress waves. Int. J. Numer. Anal. Met.35, 97-110.
505 Marketos, G., O'Sullivan, C., 2013. A micromechanics-based analytical method for wave
506 propagation through a granular material. Soil. Dyn. Earthq. Eng. 45, 25-34.

507 Miller, R.K., 1978. The effects of boundary friction on the propagation of elastic waves. Bull.
508 Seismol. Soc. Am. 68, 987-998.
509 Pyrak‐Nolte, L.J., Myer, L.R., Cook, N.G., 1990. Transmission of seismic waves across single
510 natural fractures. J. Geophys. Res.: Solid Earth (1978–2012) 95, 8617-8638.
511 Resende, R., Lamas, L., Lemos, J., Calçada, R., 2010. Micromechanical modelling of stress waves
512 in rock and rock fractures. Rock. Mech. Rock. Eng.43, 741-761.
513 Rokhlin, S., Wang, Y., 1991. Analysis of boundary conditions for elastic wave interaction with an
514 interface between two solids. J. Acoust. Soc. Am.89, 503-515.
515 Schoenberg, M., 1980. Elastic wave behavior across linear slip interfaces. J. Acoust. Soc. Am. 68,
516 1516-1521.
517 Sun, G.Z., 1988. Rock mass structure mechanics [M]. Beijing: Science Press. (in Chinese)
518 Sinha, U., Singh, B., 2000. Testing of rock joints filled with gouge using a triaxial apparatus. J.
519 Rock Mech. Min. Sci.37, 963-981.
520 Thomas, C.N., Papargyri-Beskou, S., Mylonakis, G., 2009. Wave dispersion in dry granular
521 materials by the distinct element method. Soil. Dyn. Earthq. Eng.29, 888-897.
522 Toomey, A., Bean, C.J., 2000. Numerical simulation of seismic waves using a discrete particle
523 scheme. Geophys. J. Int. 141, 595-604.
524 Verruijt, A., 2009. An introduction to soil dynamics. Springer Science & Business Media.
525 Wu, W., Li, J., Zhao, J., 2012a. Loading rate dependency of dynamic responses of rock joints at
526 low loading rate. Rock. Mech. Rock. Eng.45, 421-426.
527 Wu, W., Zhu, J., Zhao, J., 2012b. A further study on seismic response of a set of parallel rock
528 fractures filled with viscoelastic materials. Geophys. J. Int., ggs055.

529 Wu, W., Li, J., Zhao, J., 2013a. Seismic response of adjacent filled parallel rock fractures with
530 dissimilar properties. J. Appl. Geophys.96, 33-37.
531 Wu, W., Zhu, J., Zhao, J., 2013b. Dynamic response of a rock fracture filled with viscoelastic
532 materials. Eng. Geol. 160, 1-7.
533 Wu, W., Li, J., Zhao, J., 2014. Role of filling materials in a P-wave interaction with a rock fracture.
534 Eng. Geol. 172, 77-84.
535 Zamani, N., El Shamy, U., 2011. Analysis of wave propagation in dry granular soils using DEM
536 simulations. Acta. Geotech.6, 167-182.
537 Zhao, J., Cai, J., 2001. Transmission of elastic P-waves across single fractures with a nonlinear
538 normal deformational behavior. Rock. Mech. Rock. Eng.34, 3-22.
539 Zhao, J., Sun, L., Zhu, J., 2012. Modelling P-wave transmission across rock fractures by particle
540 manifold method (PMM). Geom. Geoe. 7, 175-181.
541 Zhao, X., Zhao, J., Hefny, A., Cai, J., 2006. Normal transmission of S-wave across parallel
542 fractures with Coulomb slip behavior. J. Eng. Mech.-ASCE 132, 641-650.
543 Zhu, J., Perino, A., Zhao, G., Barla, G., Li, J., Ma, G., Zhao, J., 2011. Seismic response of a single
544 and a set of filled joints of viscoelastic deformational behaviour. Geophys. J. Int.186,
545 1315-1330.
546 Zhu, J., Zhao, X., Wu, W., Zhao, J., 2012. Wave propagation across rock joints filled with
547 viscoelastic medium using modified recursive method. J. Appl. Geophys.86, 82-87.
548

549

550 ## Table captions

551 **Table 1** Micro-material properties of the particle model

552 **Table 2** Comparison of material properties of physical experiment and particle model

553

554

555

556

557

558

559

560

561

562

563

564

565

566

567

568

569

570

571

572 **Table 1 Micro-material properties of the particle model**

Rock bars		Filled layer	
k_n	1.0×10^{11} N/m	k_n	3.0×10^{8} N/m
k_s	5.0×10^{10} N/m	k_s	1.5×10^{8} N/m
Particle density	3,070 kg/m^3	*Particle density*	2,122 kg/m^3
R_{max}/R_{min}	1.6	R_{max}/R_{min}	1.6
R_{min}	0.465mm	R_{min}	0.265 mm
n_bond	1.0×10^{100} MPa	*n_bond*	0 MPa
s_bond	1.0×10^{100} MPa	*s_bond*	0 MPa
-	-	c_n	2×10^{3} N•s/m
-	-	c_s	1×10^{3} N•s/m
-	-	f	0.6

573

574

575

576

577

578

579

580

581

582

583

584 **Table 2 Comparison of material properties of physical experiment and particle model**

585

	Physical experiment	Particle model
Density of rock bars	2,650 kg/m^3	2,650 kg/m^3(continuum-equivalent)
Density of filled layer	1,592.2 kg/m^3	1,592 kg/m^3(continuum-equivalent)
P-wave velocity	4,758 m/s	4,400 m/s
Porosity of rock bars	unknown	13.7%
Porosity of filled layer	unknown	25.04%

586

587

588

589

590

591

592

593

594

595

596

597

598 ## Figure captions

599 **Fig. 1** (a) the thin layer medium model; (b) schematic view of a natural filled joint

600 **Fig. 2** Details of the Modified SHPB tests conducted by Li and Ma (2009): (a) configuration of the

601 modified SHPB tests; (b) two granite pressure bars and a sand layer sandwiched between two bars

602 **Fig. 3** The PFC2D model of the SHPB test

603 **Fig. 4** Schematic of constitutive law of normal and shear contact forces at the interface between

604 two discs

605 **Fig. 5** (a) verified model comprised of two discs; (b) comparison between the analytical result and

606 the PFC2D result.

607 **Fig. 6** The experimental result and the PFC2D result by forward fitting

608 **Fig. 7** Waveforms after half or one cycle sine stress wave propagating through a filled joint. The

609 amplitudes of the incident waves are (a). 3 m/s and (b). 6 m/s

610 **Fig. 8** Variation of transmission coefficient with the amplitude of the incident waves

611 **Fig. 9** Waveforms after two half cycle of sine pulses with different periods propagating through a

612 filled joint. (a) zero cycles of period; (b) three cycles of period

613 **Fig. 10** Variation of the transmission coefficient with the period of between two pulses

614 **Fig. 11** Variation of transmission coefficient with the thickness of the filled joints

615 **Fig. 12** Variation of transmission coefficient with frequency of the incident waves

616 **Fig. 13** Variation of transmission coefficient with dimensionless joint spacing for a half and one

617 full cycle of sine P-wave

618 **Fig. 14** Variation of transmission coefficient with dimensionless joint spacing for different

619 amplitudes of transmitted wave

620 **Fig. 15** Snapshots at different times of the deformation of the filled joint (a) a half cycle of and (b)

621 one cycle of sin P-wave is applied respectively

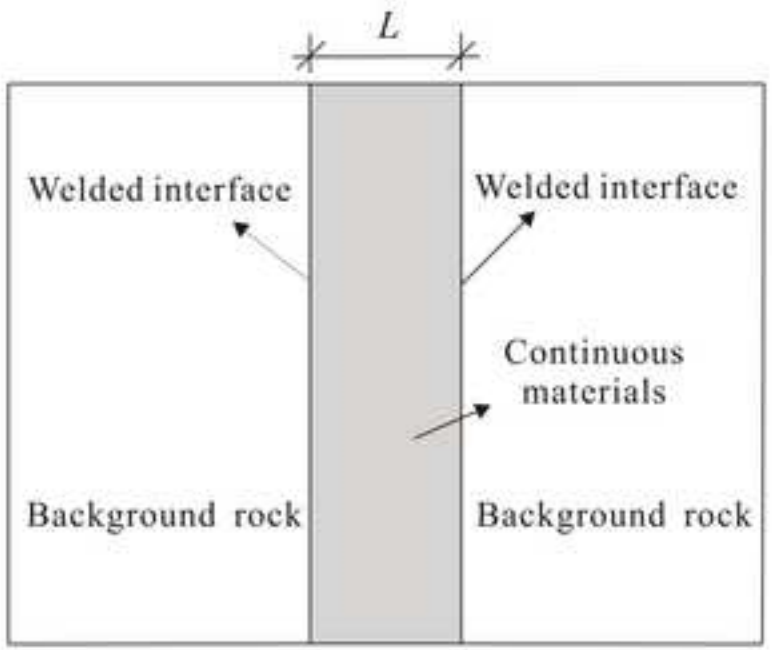

(a) Thin layer medium model

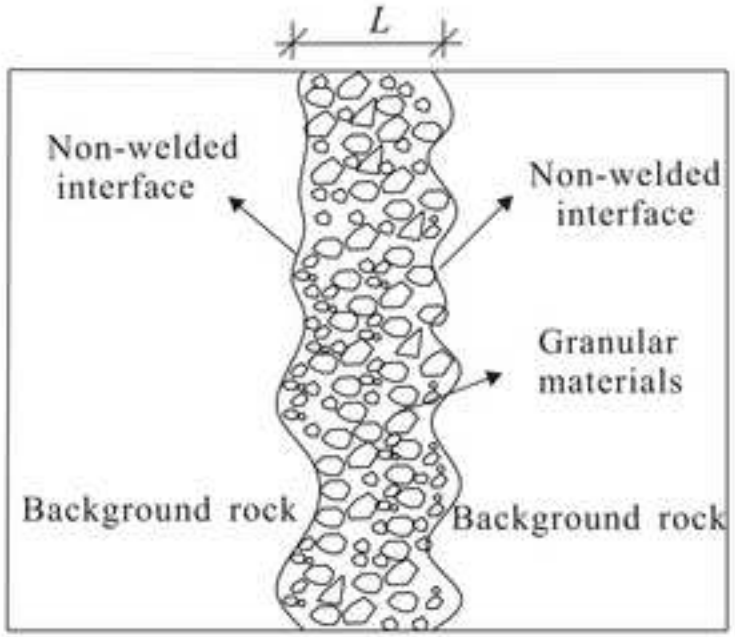

(b) Schematic view of a natural filled joint

a

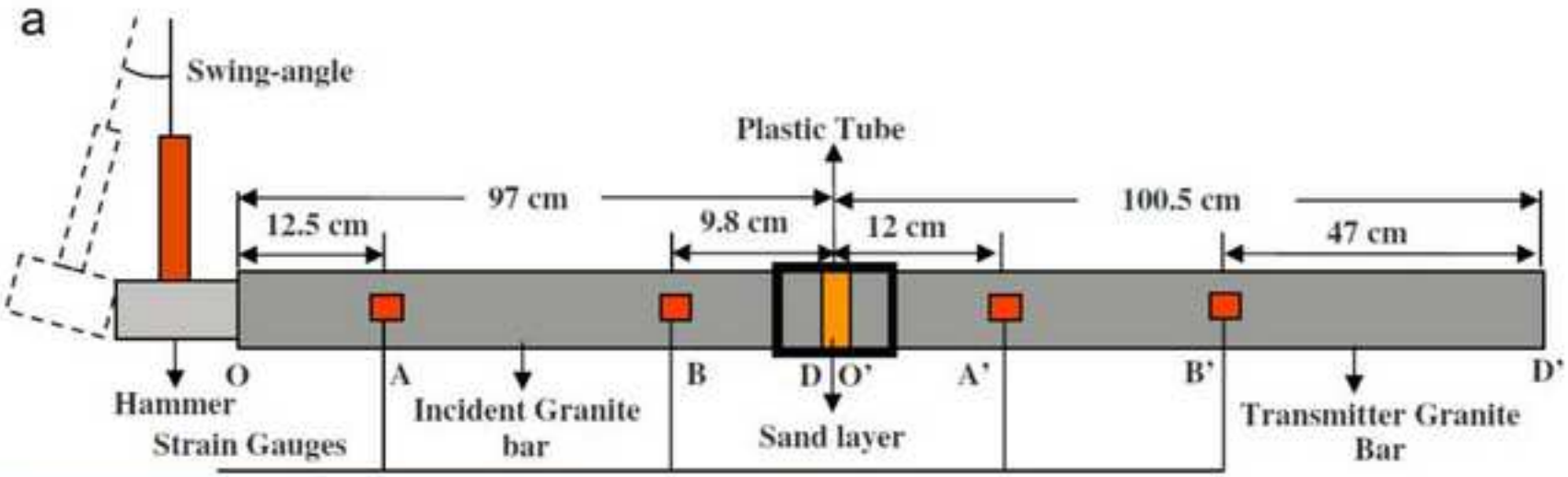

b

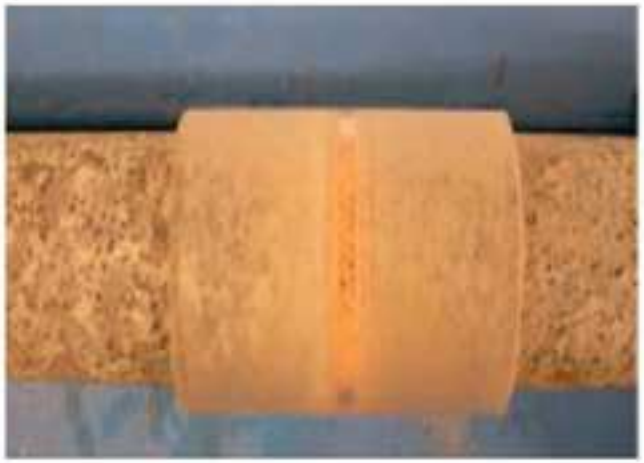

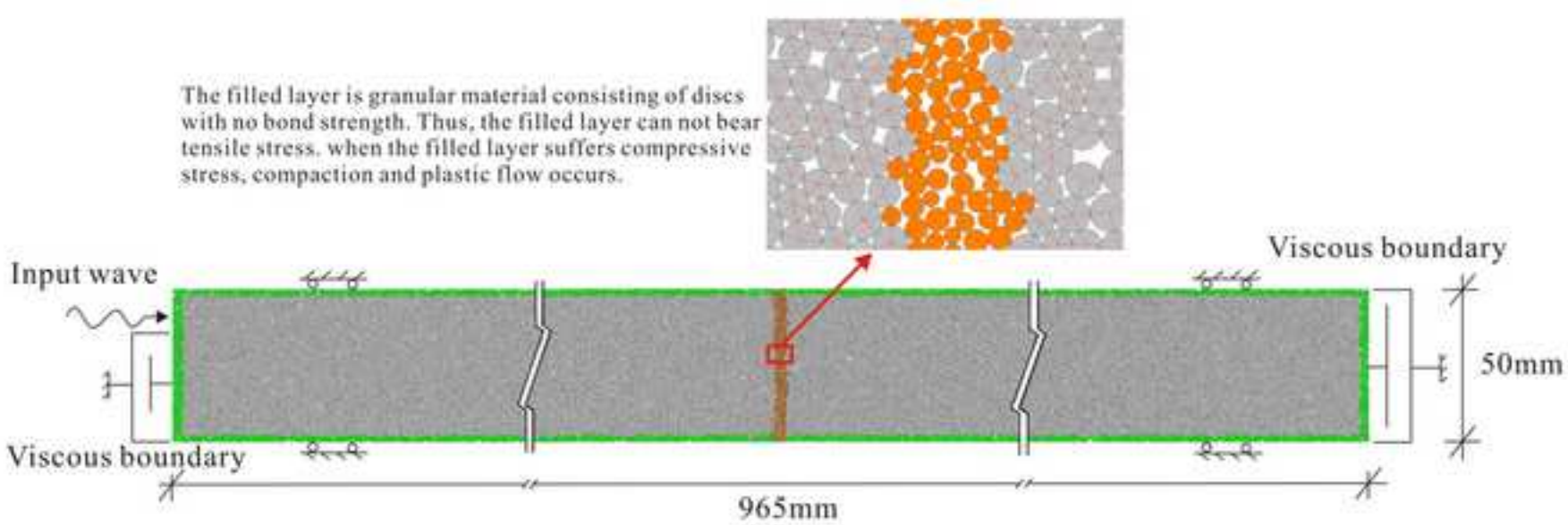

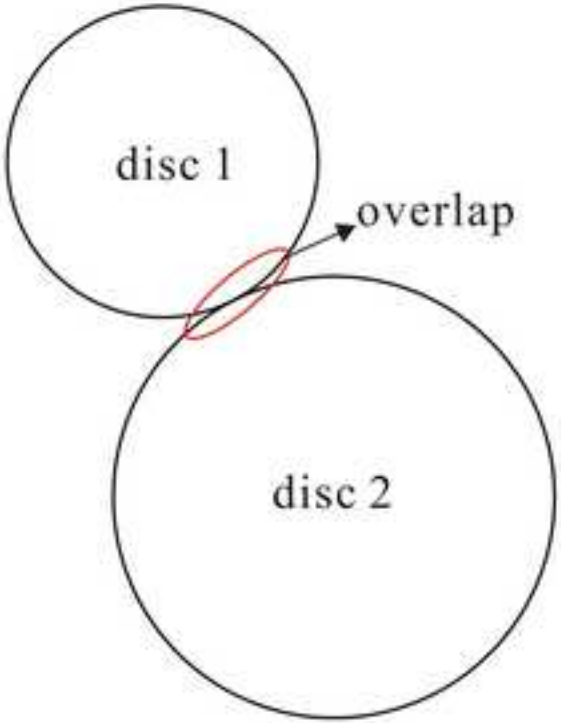

(a) the contact and overlap of two discs

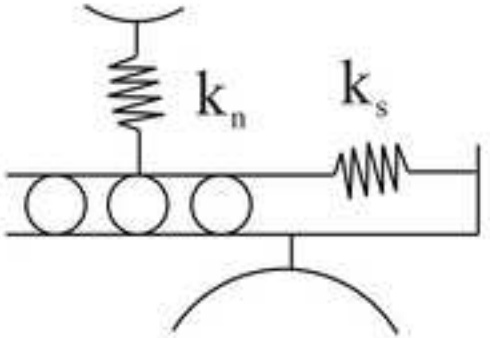

(b) disc contact model for rock

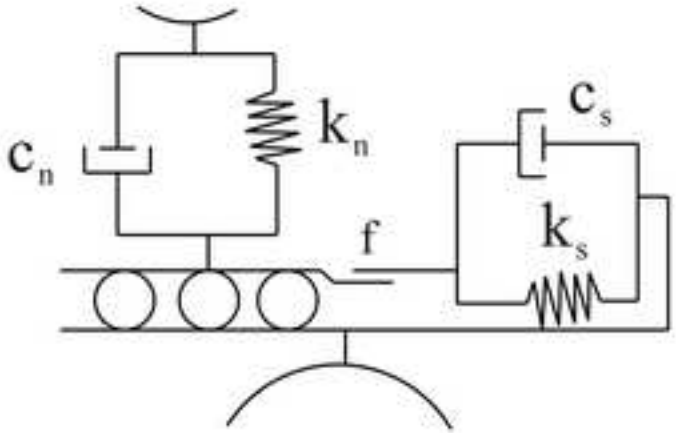

(c) disc contact model for filled granular material

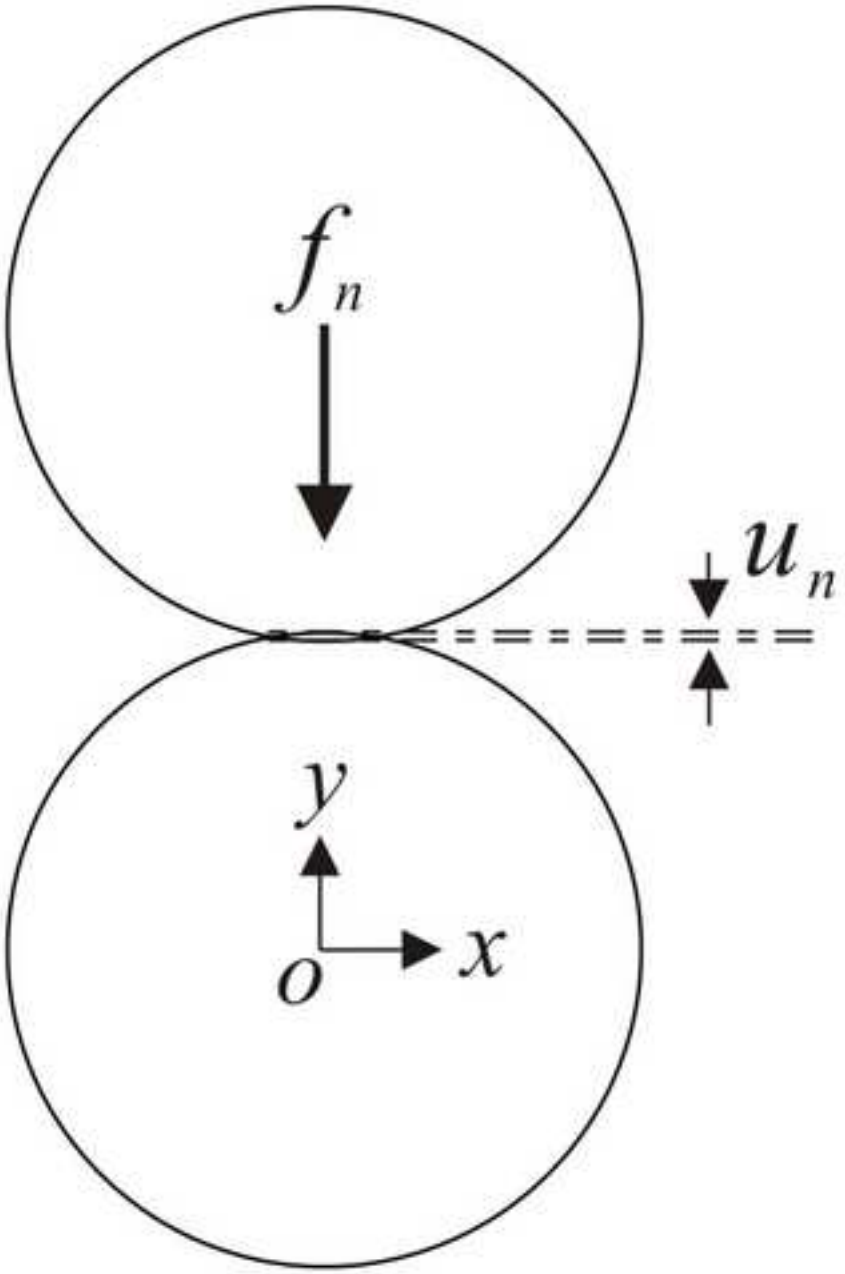

(a)

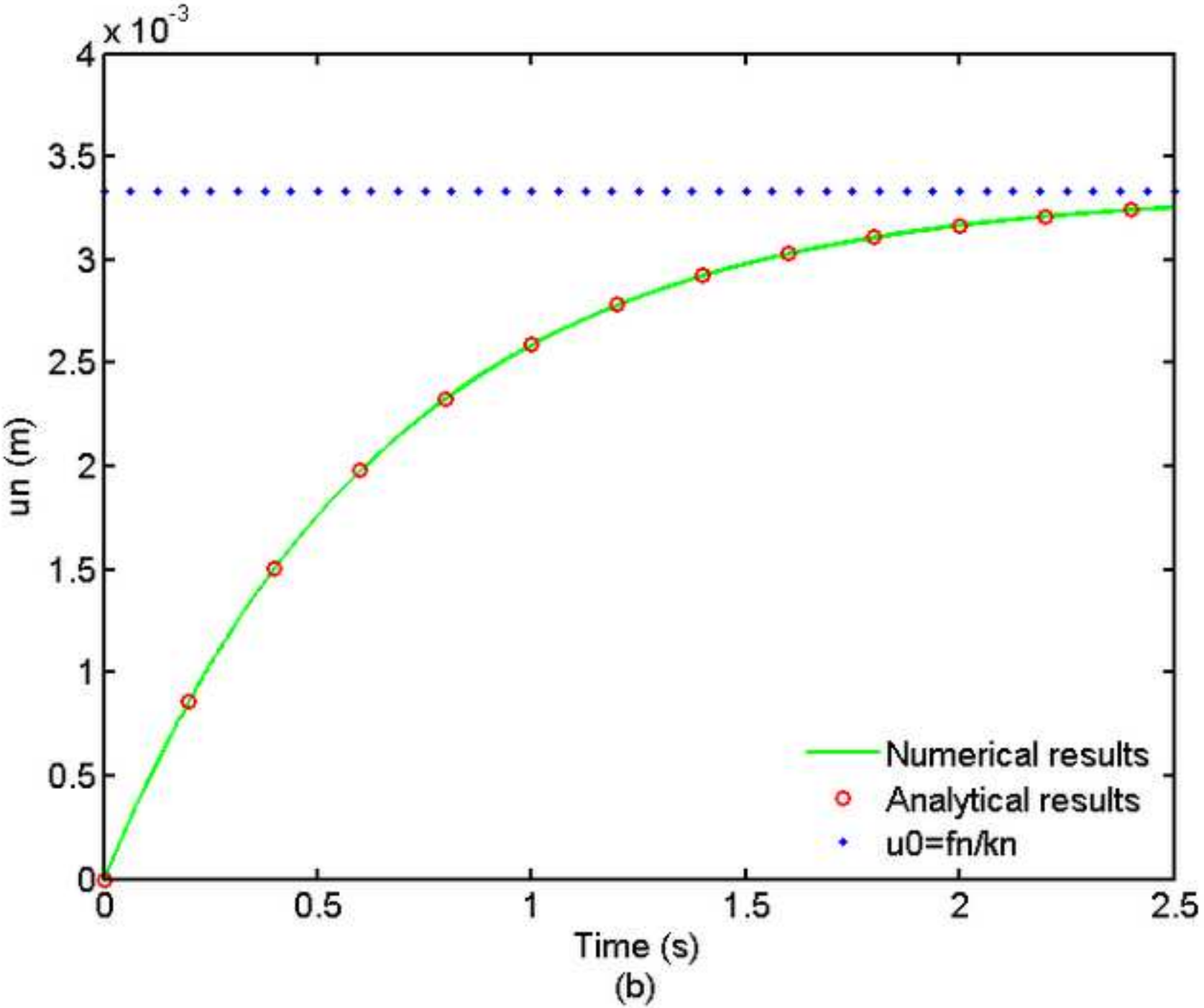

(b)

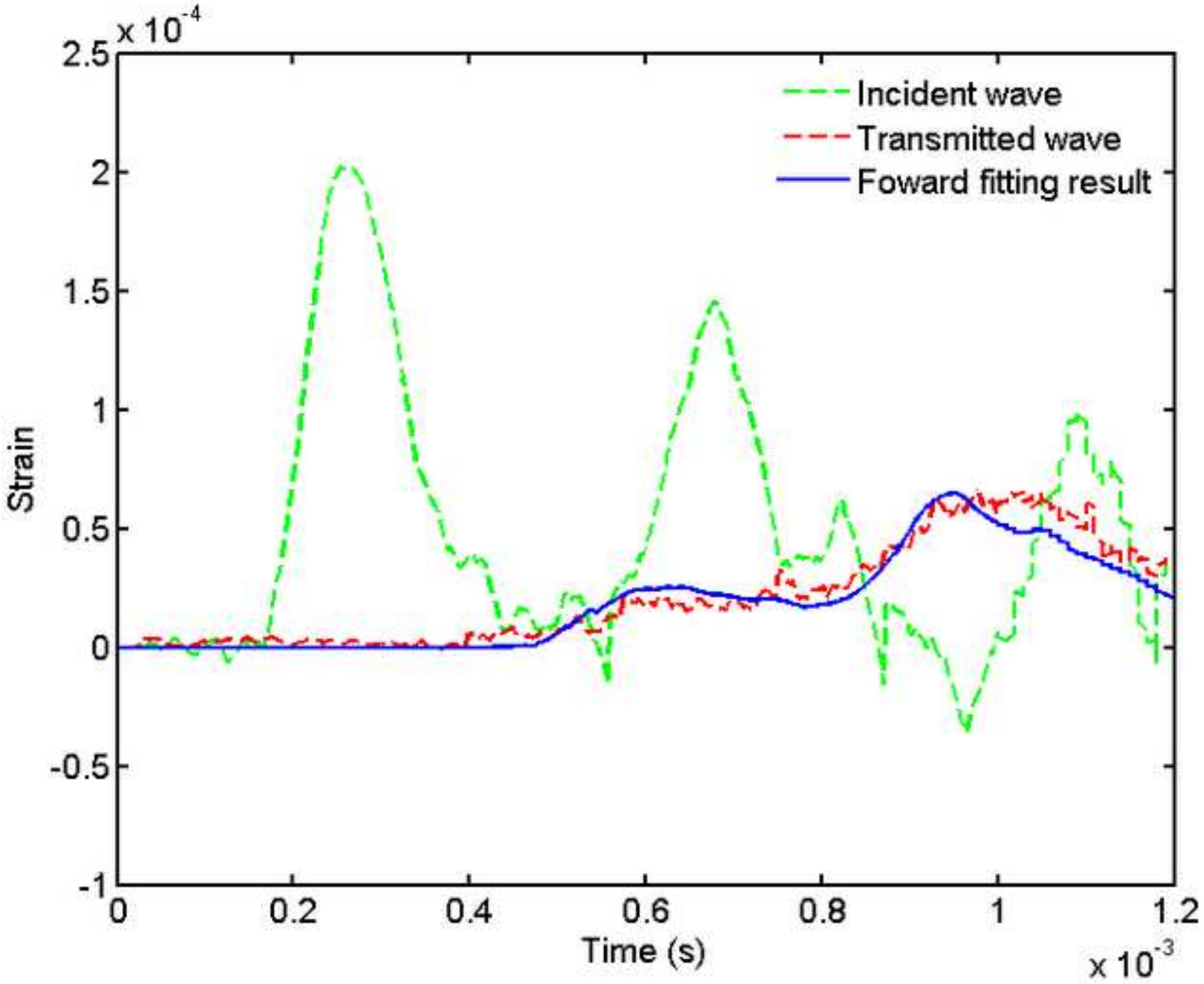

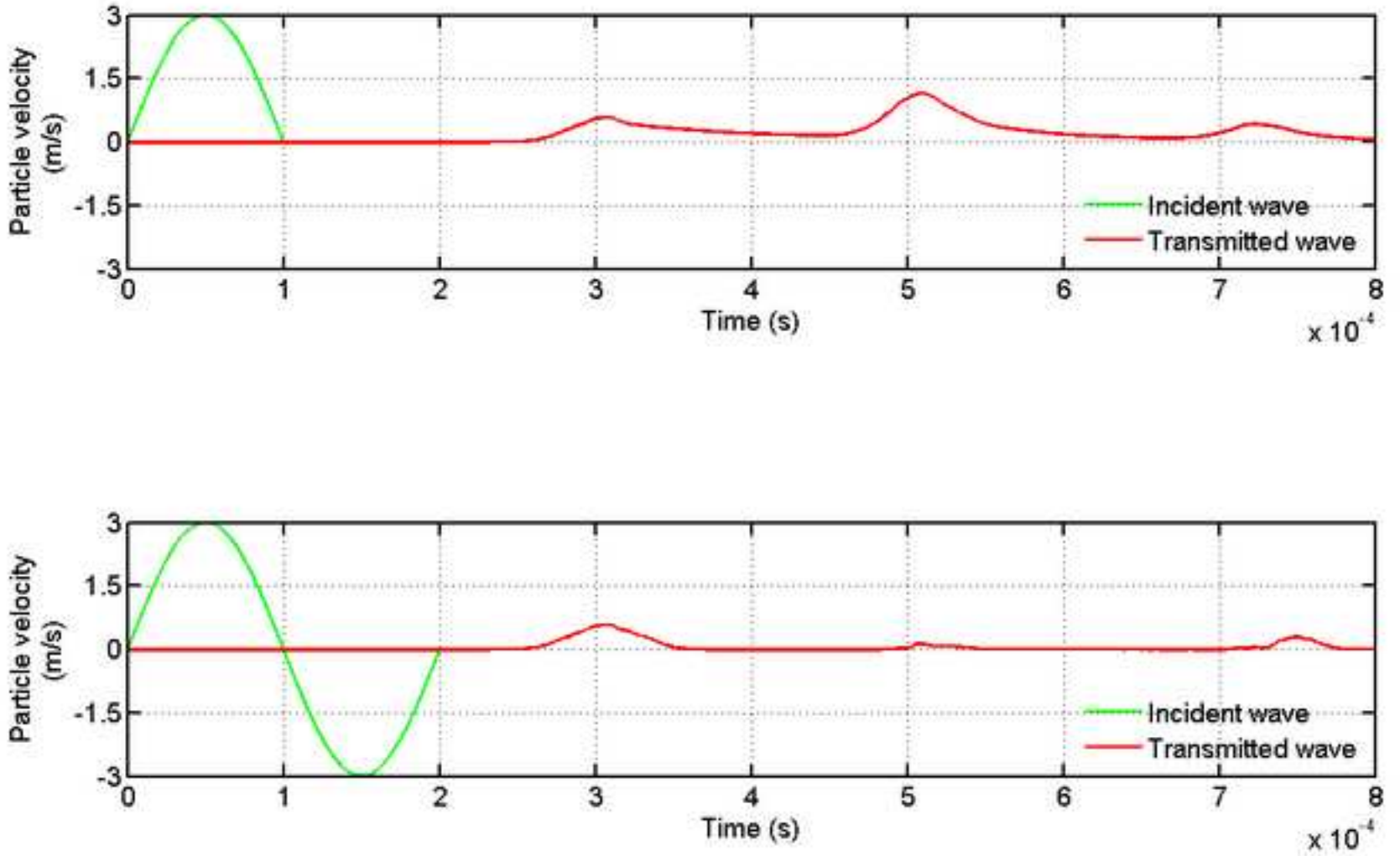

(a) Amplitude of 3 m/s

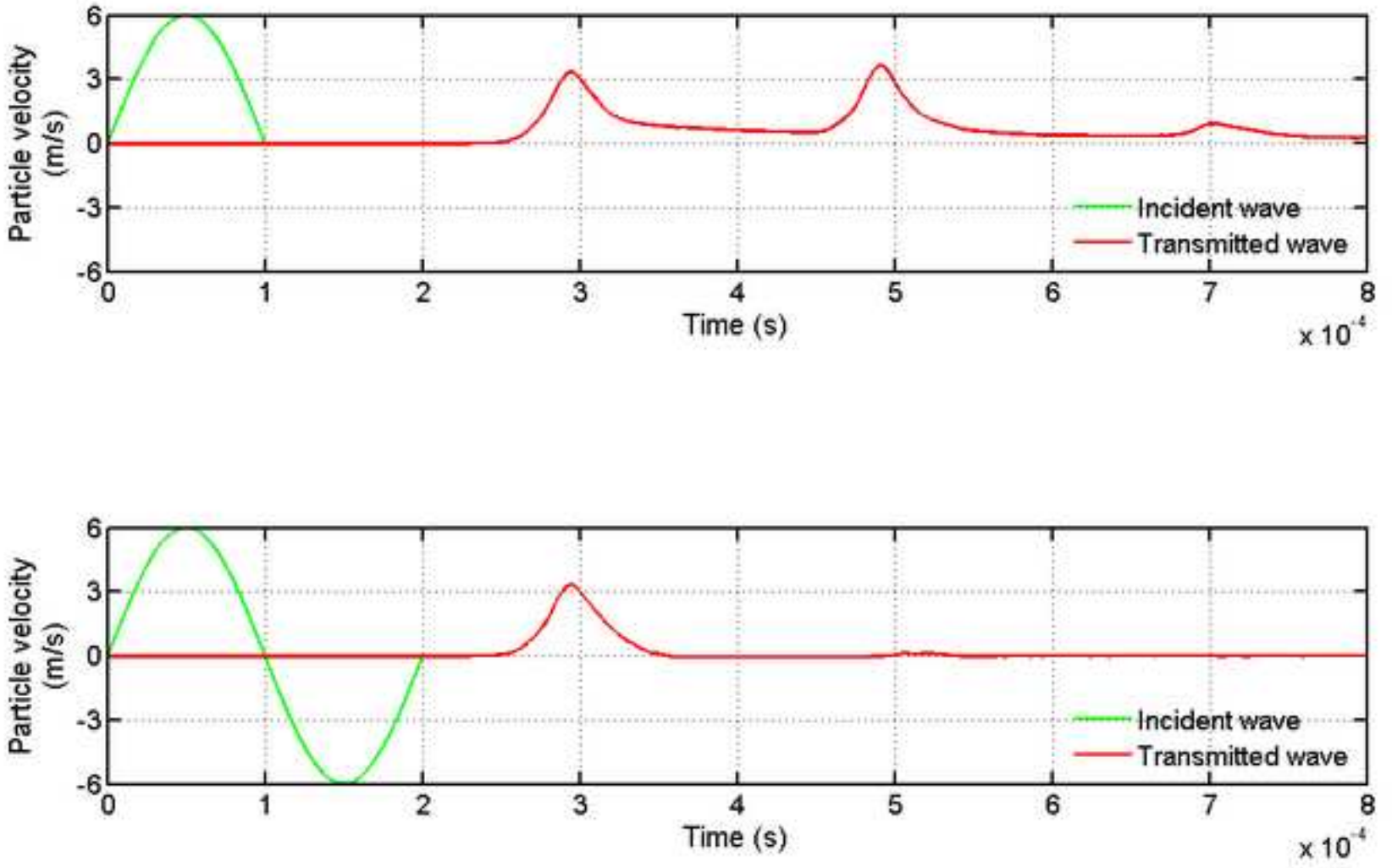

(b) Amplitude of 6 m/s

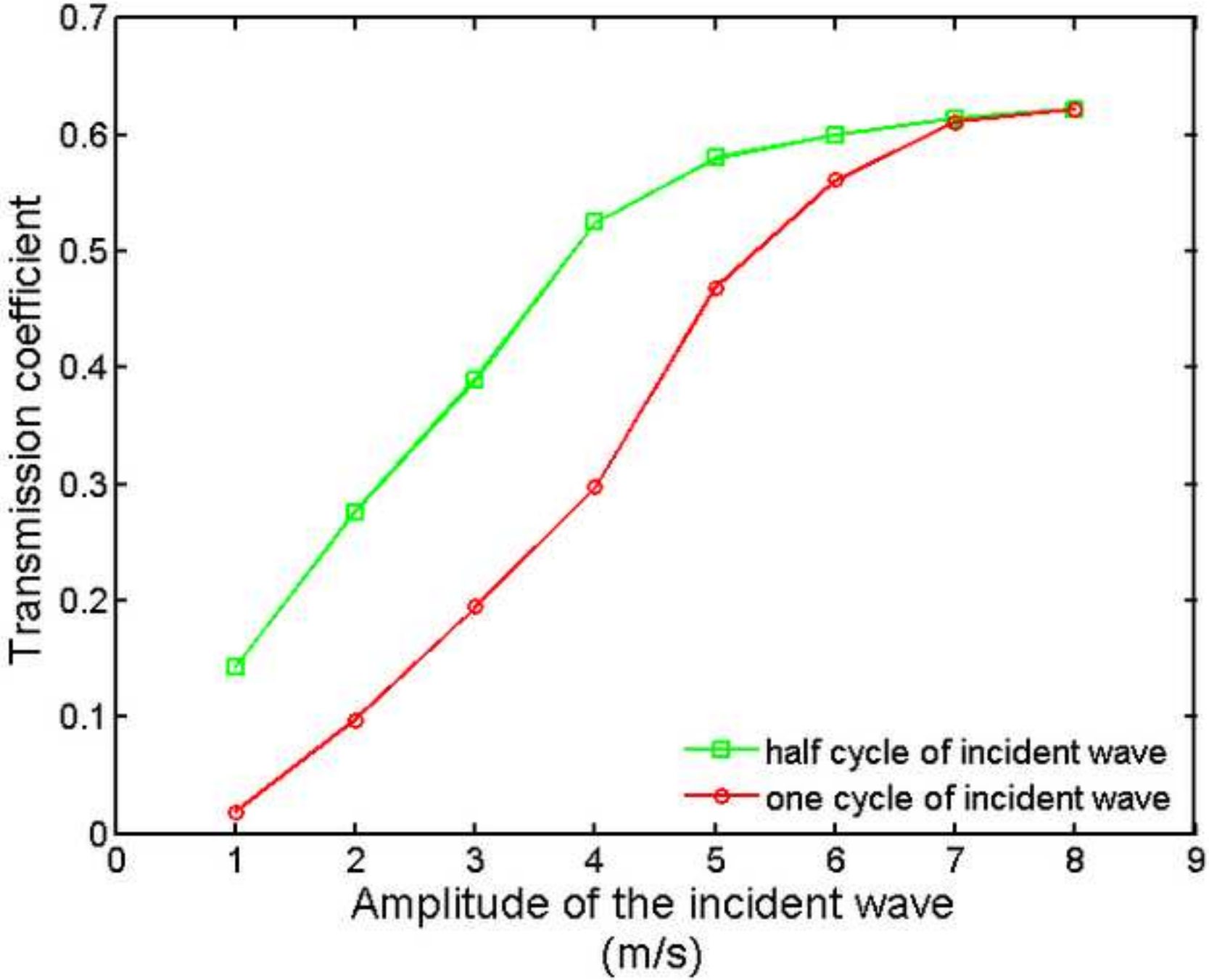

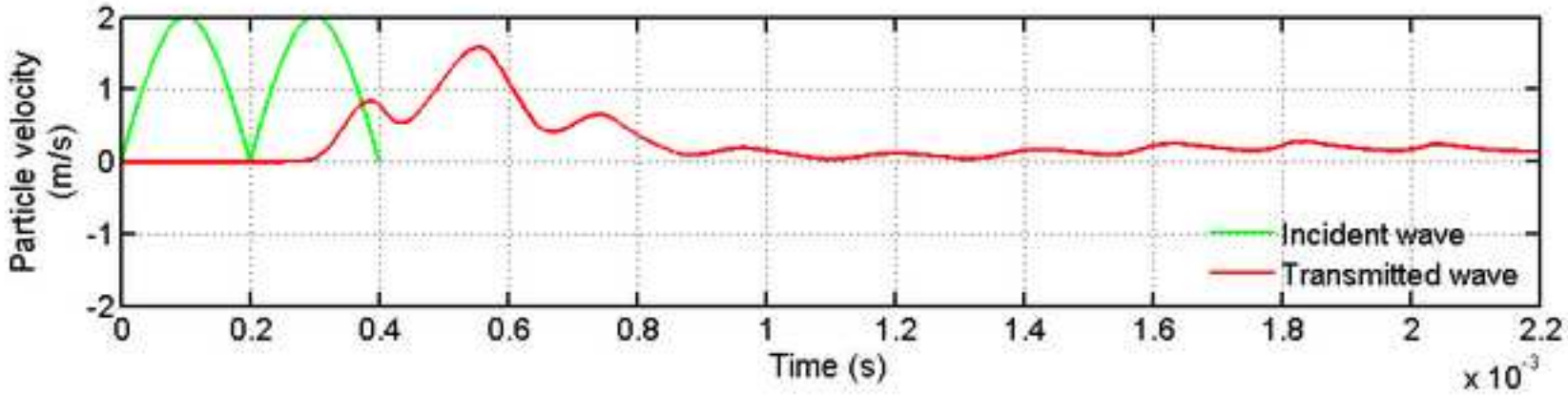

(a) Zero cycle of interval

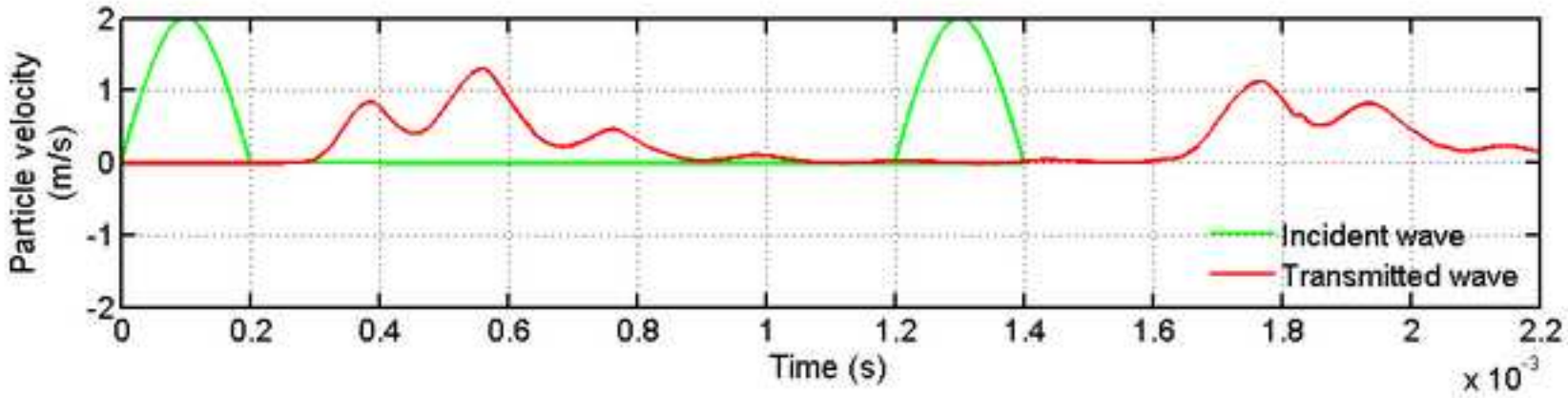

(b) Three cycles of interval

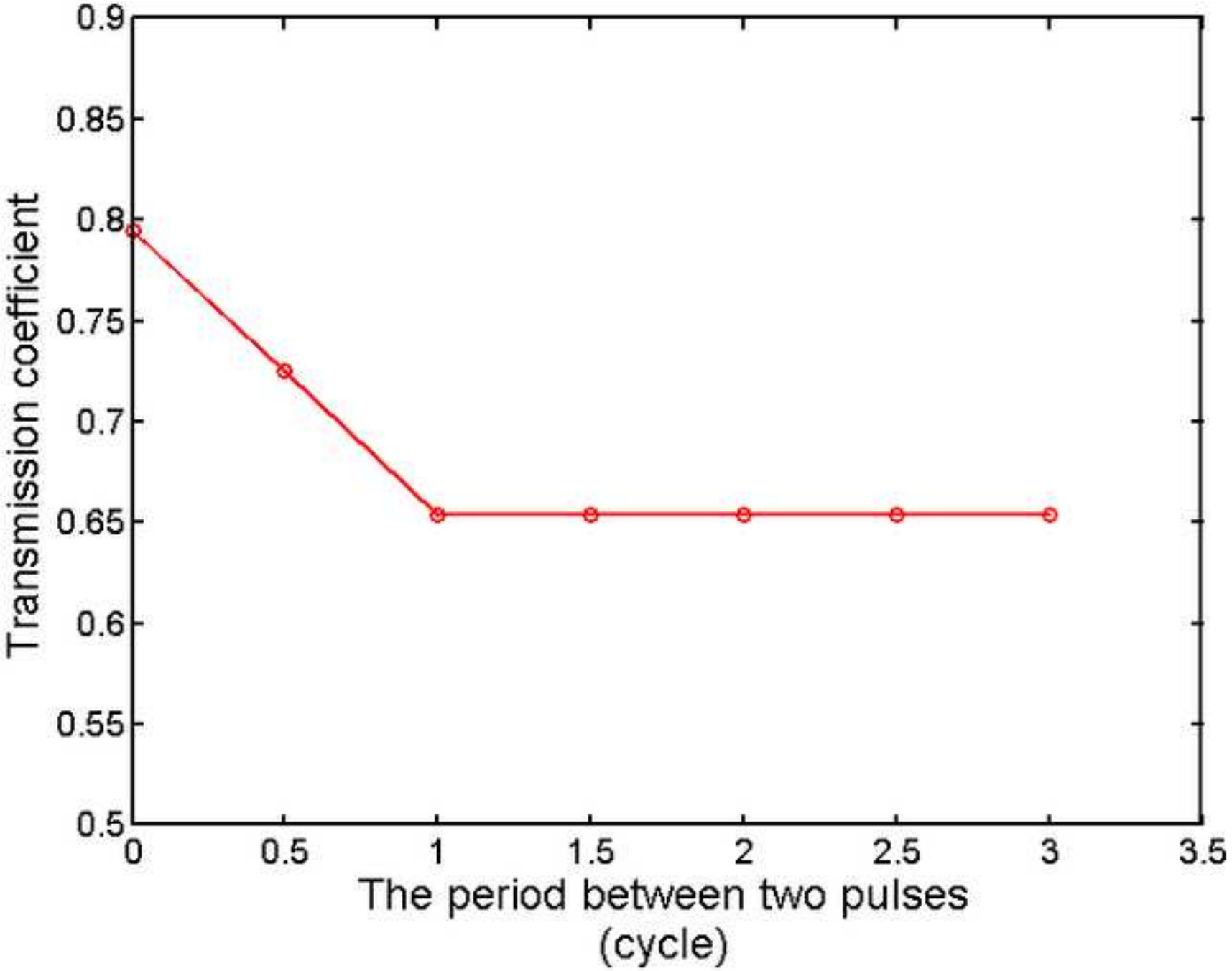

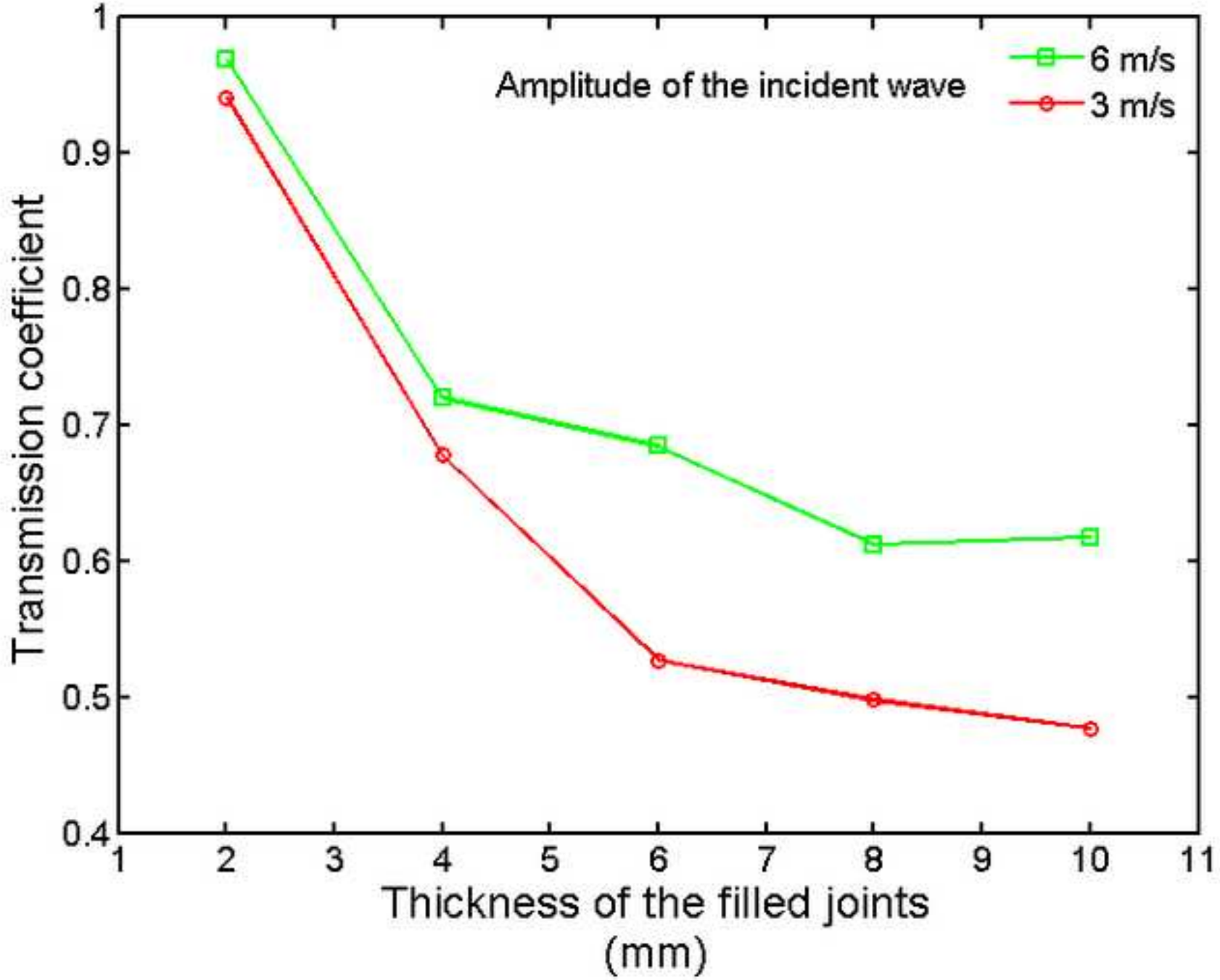

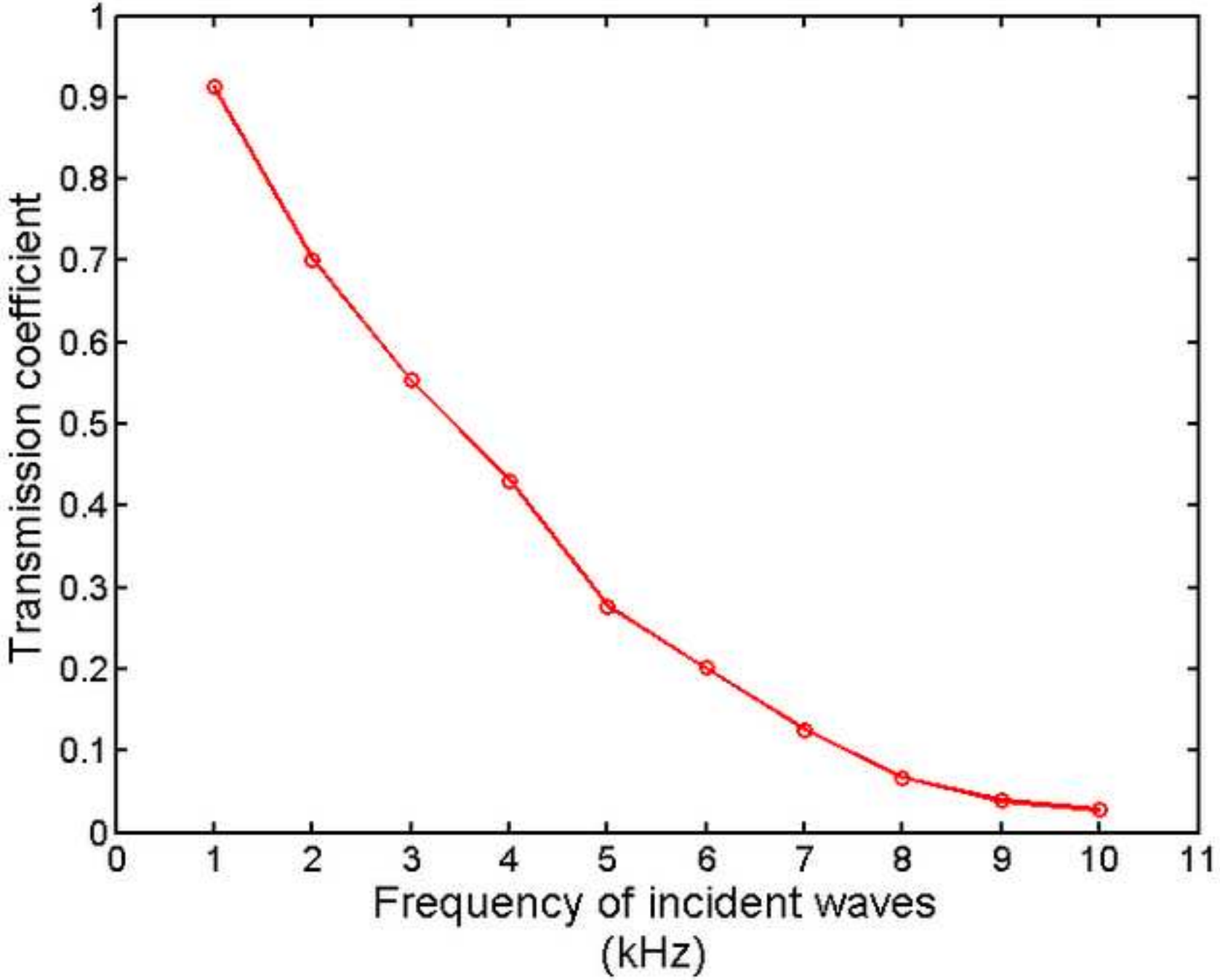

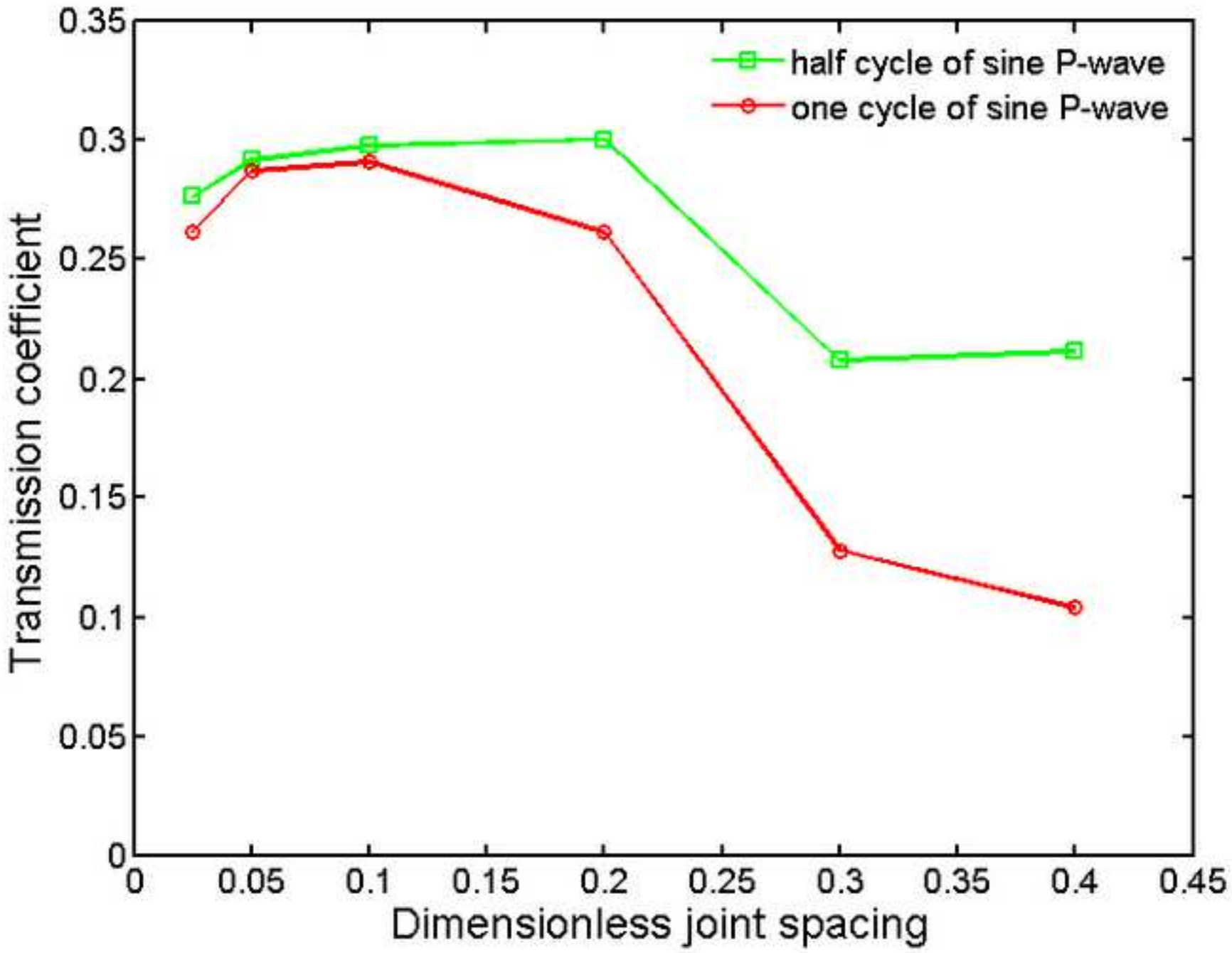

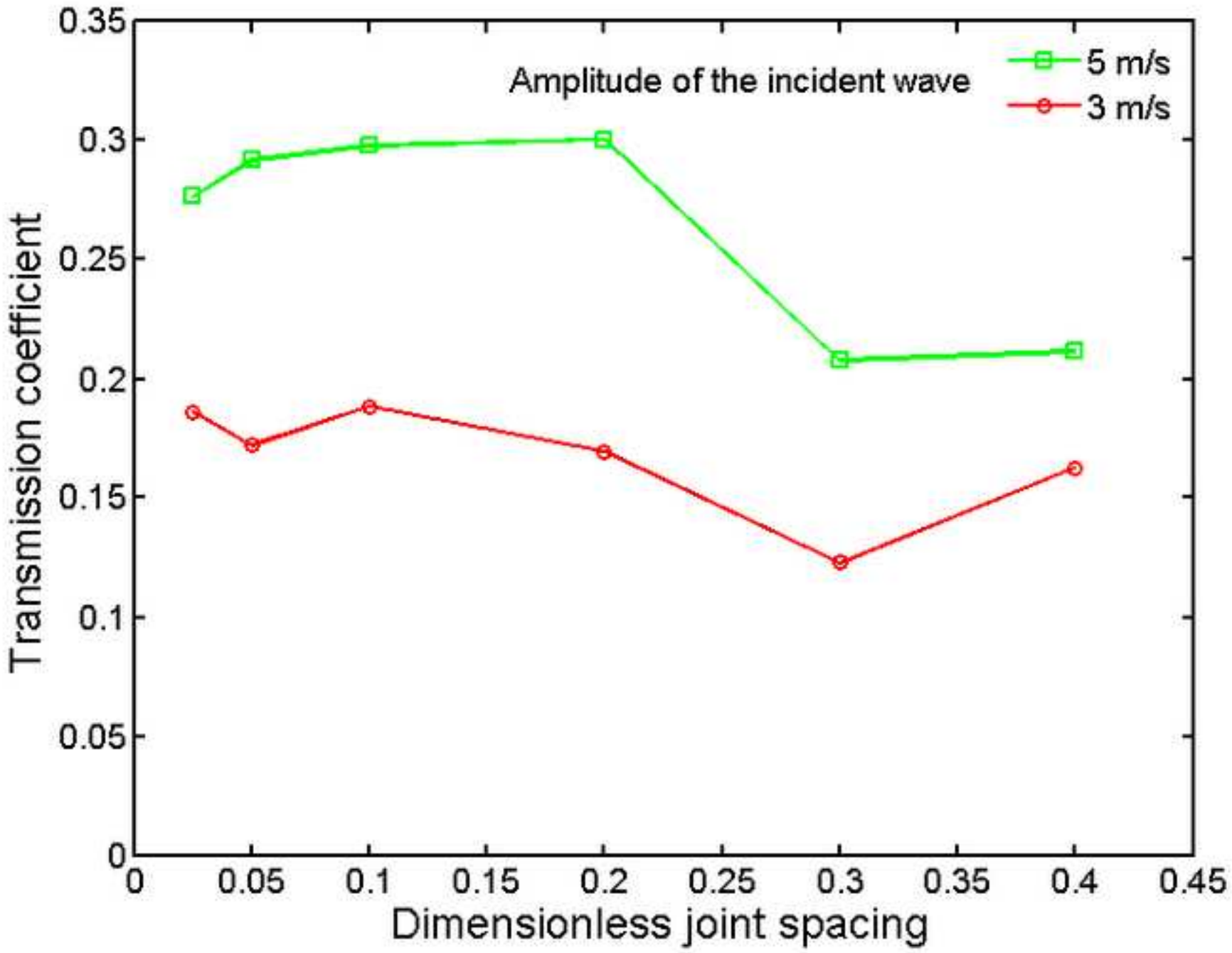

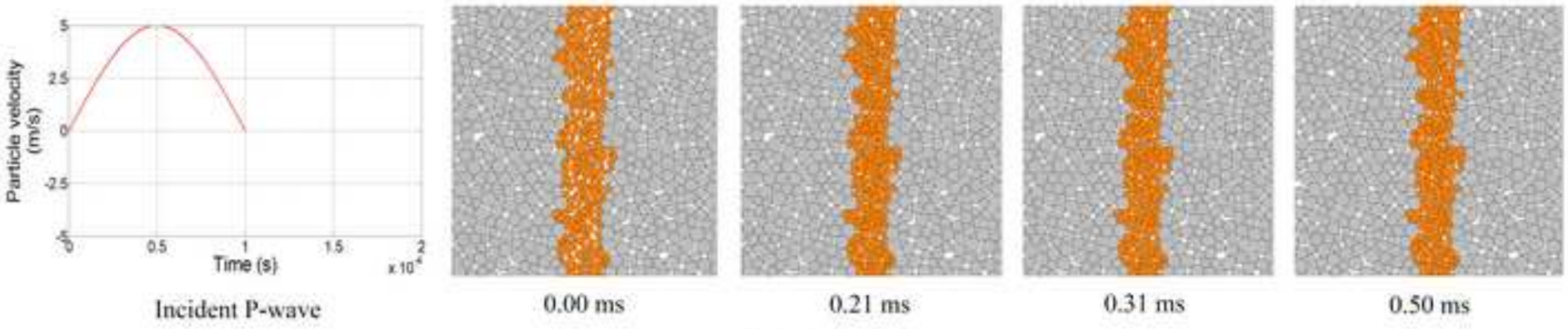

(a) Case of half cycle of sine wave

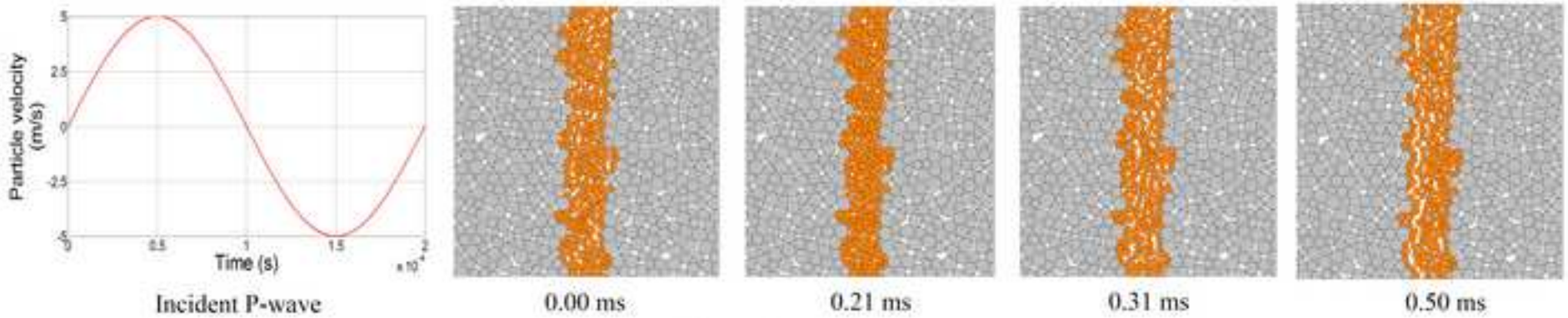

(b) Case of one cycle of sine wave

Highlights (for review)

Highlights

► The Kelvin viscous-elastic contact model is developed with C++ code in PFC2D 3.10.

► The developed model can simulate the stress wave propagation.

►The effect of tensile stress and the loading history were considered respectively.

►The microscopical process of the filled layer under varied loading mode was examined .